

Fluctuations of the order parameter in an $SU(N_c)$ effective model

Pok Man Lo^{✉,*}, Krzysztof Redlich, and Chihiro Sasaki

Institute of Theoretical Physics, University of Wrocław, PL-50204 Wrocław, Poland



(Received 4 February 2021; accepted 2 April 2021; published 28 April 2021)

We investigate features of the deconfinement phase transition in an $SU(N_c)$ gauge theory as revealed by fluctuations of the order parameter. The tool of choice is an effective model built from one-loop expressions of the field determinants of gluon and ghost, in the presence of a Polyakov loop background field. We show that the curvature masses associated with the Cartan angles, which serve as a proxy to study the A_0 -gluon screening mass, show a characteristic dip in the vicinity of the transition temperature. The strength of the observables, which reflects a competition between the confining and the deconfining forces, is sensitive to assumptions of dynamics, and thus provides an interesting link between the $Z(N_c)$ vacuum structure and the properties of gluon and ghost propagators.

DOI: [10.1103/PhysRevD.103.074026](https://doi.org/10.1103/PhysRevD.103.074026)

I. INTRODUCTION

In this work we study the fluctuations of the order parameter in an $SU(N_c)$ gauge theory within an effective model. Unlike the order parameter, these observables are finite and temperature dependent even in the confined phase, thus providing important diagnostic information about the mechanism of deconfinement phase transition, and the properties of gluons (and ghosts) in relation to the structure of $Z(N_c)$ vacuum.

Even when powerful numerical methods such as lattice QCD (LQCD) are available to perform *ab initio* calculations of the full theory [1–3], it is instructive, and sometimes essential, to work on an effective model description of a dynamical system. First of all, it provides clear links between the observables and the underlying symmetry. Second, it enables straightforward application of the model to other extreme conditions [4,5], or as a building block to study further coupling to other dynamical fields [6–11].

A common strategy to constructing an effective potential is via a polynomial of the order parameter field [12–14], i.e., the Ginzburg-Landau theory. Symmetry restricts the kind of terms that can appear in the potential. The coefficients are generally smooth functions of temperatures (and other external fields), which need to be separately determined, e.g., by fitting observables to LQCD results.

While a polynomial type potential is convenient to work with, the relation between model parameters and the

properties of the underlying gluons (and ghosts) is not transparent. In this study, we employ an effective potential built from one-loop expressions of the field determinants of gluon and ghost described in Ref. [15]. (See also Ref. [16].) The model naturally describes both the confined and the deconfined phases, as related to the spontaneous breaking of $Z(N_c)$ symmetry. In particular, the ghost term gives a confining, i.e., $Z(N_c)$ restoring, potential. The effective model, as a tool, allows us to gain insights into the interplay between vacuum structure and dynamics.

The thermal properties of a pure gauge system have been analyzed previously by effective models [13,14,16–23]. However, features of gluons in the confined phase are usually not examined, and the importance of fluctuation observables [24] has not been fully realized. We therefore focus on these observables in this work and study how features of deconfinement manifest through them. We also use this opportunity to clarify the connection of these observables to eigenvalues of the Polyakov loop operator in a matrix model [13,17,18]. We show that the curvature masses associated with the Cartan angles, which serve as a proxy to study the A_0 -gluon screening mass, shows a characteristic trend of a rapid drop in the vicinity of transition temperature T_d . Such a behavior is traceable to the competing effect of $Z(3)$ restoring (confining) and $Z(3)$ breaking (deconfining) forces. The strength of the masses is sensitive to the assumptions made on the dynamical properties of gluon and ghost propagators. Finally we present a possible relation between the glueball mass and T_d suggested by the model.

II. GROUP STRUCTURE OF $SU(N_c)$

The Polyakov loop operator in the fundamental representation, after a diagonalizing unitary transformation, can be expressed by the N_c eigenphases \vec{q} :

*pokman.lo@uwr.edu.pl

Published by the American Physical Society under the terms of the [Creative Commons Attribution 4.0 International license](https://creativecommons.org/licenses/by/4.0/). Further distribution of this work must maintain attribution to the author(s) and the published article's title, journal citation, and DOI. Funded by SCOAP³.

$$\hat{\ell}_F = \text{diag}(e^{iq_1}, e^{iq_2}, \dots, e^{iq_{N_c}}). \quad (1)$$

The first $N_c - 1$ phases may be taken as independent, and unitarity is enforced by requiring

$$q_{N_c} = - \sum_{j=1}^{N_c-1} q_j. \quad (2)$$

Alternatively, the angles can be expressed in terms of the $N_c - 1$ group angles of the maximal $Z(N_c)$ Cartan subgroup, $(\gamma_j$'s),

$$\vec{q} = \sum_{j=1}^{N_c-1} \gamma_j \vec{v}_j, \quad (3)$$

where $\{\vec{v}_j\}$ is a set of basis vectors, each being an N_c dimensional vector with its sum of elements zero. The order parameter field is obtained from a trace of $\hat{\ell}_F$,

$$\ell = \frac{1}{N_c} \text{Tr} \hat{\ell}_F. \quad (4)$$

For $N_c \geq 3$, the order parameter is complex, and one can explore its real and imaginary parts:

$$\begin{aligned} \ell &= X + iY, \\ X &= \frac{1}{N_c} \sum_{j=1}^{N_c} \cos(q_j), \\ Y &= \frac{1}{N_c} \sum_{j=1}^{N_c} \sin(q_j). \end{aligned} \quad (5)$$

Note that X, Y are regarded as a scalar function of the $N_c - 1$ Cartan angles $\vec{\gamma}$'s.

To study the fluctuations of the order parameter in an effective model, we need to perform X, Y -field derivatives of a potential. Equation (5) provides a connection between these derivatives with those acting on γ_j 's,

$$\begin{aligned} \frac{d}{dX} &= \sum_{j=1}^{N_c-1} C_{1j}(\vec{\gamma}) \frac{d}{d\gamma_j}, \\ \frac{d}{dY} &= \sum_{j=1}^{N_c-1} C_{2j}(\vec{\gamma}) \frac{d}{d\gamma_j}, \end{aligned} \quad (6)$$

where the $2 \times (N_c - 1)$ matrix C is obtained by (left) inverting the transpose of the Jacobian J :

$$\begin{aligned} J &= \frac{\partial\{X, Y\}}{\partial\{\gamma_1, \gamma_2, \dots, \gamma_{N_c-1}\}}, \\ C &= [J^t]^{-1}. \end{aligned} \quad (7)$$

Finally, starting with a potential expressed in terms of the Cartan angles, $U(\vec{\gamma})$, the susceptibilities can be computed by forming the curvature matrix $\bar{U}^{(2)}$ [10,25,26]

$$\bar{U}^{(2)} = \frac{1}{T^4} \begin{pmatrix} \frac{\partial^2 U}{\partial X \partial X} & \frac{\partial^2 U}{\partial X \partial Y} \\ \frac{\partial^2 U}{\partial Y \partial X} & \frac{\partial^2 U}{\partial Y \partial Y} \end{pmatrix}. \quad (8)$$

The various (X, Y) -field derivatives are calculated according to Eq. (6). Inverting the curvature matrix gives

$$T^3 \tilde{\chi} = (\bar{U}^{(2)})^{-1}, \quad (9)$$

with

$$\begin{aligned} T^3 \chi_L &= T^3 \tilde{\chi}_{11}, \\ T^3 \chi_T &= T^3 \tilde{\chi}_{22}. \end{aligned} \quad (10)$$

Note that the notions of longitudinal and transverse directions [24] correspond to real and imaginary components along the real line, but this is not so for other $Z(N_c)$ vacua.

To illustrate the computation of fluctuations, we consider a schematic effective potential (model A) of the form

$$U = U_{\text{conf.}} + U_{\text{glue}}, \quad (11)$$

where the confining part is modeled by the group invariant measure H [27],

$$U_{\text{conf.}} = -\frac{b}{2} T \ln H. \quad (12)$$

This potential is confining in the sense that it tends to drive the system toward the $Z(N_c)$ symmetric vacuum ($\ell = 0$). The deconfining part, which prefers the spontaneously broken $Z(N_c)$ vacuum, is modeled as

$$\begin{aligned} U_{\text{glue}} &= n_{\text{glue}} T \int \frac{d^3 k}{(2\pi)^3} \\ &\times \text{Tr}_A \ln(I - \hat{\ell}_A e^{-\beta E_A(k)}), \end{aligned} \quad (13)$$

with $E_A(k) = \sqrt{k^2 + m_A^2}$. In Sec. IV, we shall investigate some alternative forms of the potential and discuss issues of gauge dependence and inclusion of wave function renormalizations.

As we are mainly interested in studying the influence from group structure, we shall keep the model parameters as simple as possible. In fact, we shall start with the parametrization: $b = (0.1745 \text{ GeV})^3$, $n_{\text{glue}} = 2$, and $m_A \approx 0.756 \text{ GeV}$.¹ Two group structures appear in this schematic model: the adjoint operator $\hat{\ell}_A$ and the group invariant measure H . It is useful to express them in terms of the eigenphases. For the former,

¹Such a value of gluon mass ($\approx 0.7 \text{ GeV}$) is supported by calculations in different gauges. We have also checked that using the Gribov dispersion relation $E(k) = \sqrt{k^2 + m_A^4/k^2}$ [28] or imposing a UV cutoff for $m_A \rightarrow m_A e^{-k^2/\Lambda^2}$ [29] does not lead to significant differences in the observables studied.

$$\hat{\ell}_A = \text{diag}(e^{iQ_1}, e^{iQ_2}, \dots, e^{iQ_{N_c^2-1}}), \quad (14)$$

with

$$\vec{Q} = (0, \dots, 0; q_j - q_k, -(q_j - q_k)), \quad (15)$$

for $j < k$, $j, k = 1, 2, \dots, N_c$. The adjoint angles are constructed from the root system [13,30], classified into Cartan and non-Cartan parts: (a) $N_c - 1$ zeros, representing the identity matrix element in $\hat{\ell}_A$; (b) $N_c(N_c - 1)/2$ pairs of $q_i - q_j$'s for $i > j$ and terms with the opposite sign.

An intuitive way to understand the form of potential Eq. (13) is to realize that the adjoint derivative operator for the gluon field, in the presence of a diagonal background field $\hat{q} = i\beta g \bar{A}_0 = \beta g \bar{A}_4$, reads

$$\bar{D}_\mu^{\text{adj}} \mathbf{M} = \partial_\mu \mathbf{M} + \delta_{\mu 0} \frac{1}{\beta} [\hat{q}, \mathbf{M}]. \quad (16)$$

The adjoint operator acts on an arbitrary $SU(N_c)$ matrix \mathbf{M} , and the latter has $N_c^2 - 1$ independent entries. As \hat{q} is diagonal, the ij th component of the commutator $[\hat{q}, \mathbf{M}]$ is given by [31,32]

$$(q_i - q_j) \mathbf{M}_{ij}. \quad (17)$$

For $i \neq j$, the multiplying factors are exactly the nontrivial entries of the adjoint angles \vec{Q} in Eq. (15). The remaining N_c diagonal elements of \mathbf{M} , of which $N_c - 1$ are independent, are multiplied by 0, i.e., the Cartan part of \vec{Q} . The effects of the background field is thus similar to introducing an imaginary chemical potential for the $N_c^2 - 1$ independent components. In particular, the gauge field determinant can be constructed:

$$\begin{aligned} \text{Tr} \ln \bar{D}_{\text{adj}}^2 &= \sum_a V \sum_{\vec{k}} \ln \left(\left(\omega_n + \frac{Q_a}{\beta} \right)^2 + (\vec{k})^2 \right) \\ &= 2V \int \frac{d^3 k}{(2\pi)^3} \text{Tr}_A \ln (I - \hat{\ell}_A e^{-\beta k}) + (T=0), \end{aligned} \quad (18)$$

where \sum denotes a Matsubara sum over the bosonic frequencies and an integral over momenta. From now on, we shall retain only the finite temperature piece. Equation (13) is its simple extension to introducing a finite gluon mass.

Another group structure of interest is the invariant measure. This can also be expressed in terms of the eigenphases q_j 's via

$$\begin{aligned} H &= \prod_{j>k} |e^{iq_j} - e^{iq_k}|^2 \\ &= \prod_{j>k} 4 \sin^2 \left(\frac{q_j - q_k}{2} \right). \end{aligned} \quad (19)$$

Note that there are $N_c(N_c - 1)/2$ pairs of ($j > k$) in the product. A fact that would prove useful later is the construction of the (logarithm of) invariant measure from

$$\ln H = \text{Tr}'_A \ln (I - \hat{\ell}_A), \quad (20)$$

where Tr' denotes the partial trace over the non-Cartan roots to avoid irrelevant divergences from vanishing elements. Hence the effective potential can be expressed as

$$U_{\text{conf.}} = -\frac{b}{2} T \text{Tr}'_A \ln (1 - \hat{\ell}_A), \quad (21)$$

with $\hat{\ell}_A$ in Eqs. (14) and (15). This establishes that an invariant measure term behaves as the glue potential (13) with $E_A(k) \rightarrow 0$, but of the opposite sign, and should be formally understood as a ghost contribution [33,34].

Here we explicitly work out the case for $N_c = 2, 3, 4$.

A. $N_c = 2$

In this case there is only a single independent eigenphase $\vec{q} = (q_1, -q_1)$ for the Polyakov loop operator $\hat{\ell}_F$,

$$\hat{\ell}_F = \text{diag}(e^{iq_1}, e^{-iq_1}), \quad (22)$$

and the order parameter field is purely real,

$$\ell = \cos q_1. \quad (23)$$

The adjoint angles can be constructed

$$\vec{Q} = (0; 2q_1, -2q_1), \quad (24)$$

and from Eq. (20) the invariant measure works out to be

$$\begin{aligned} H(q_1) &= 4 \sin^2 q_1 \\ &= 4(1 - \ell^2). \end{aligned} \quad (25)$$

The same result may be obtained from a slightly different starting point. Consider the parametrization of $SU(2)$ matrices $\{u\}$ by (a_0, \vec{a}) via

$$u = a_0 I + i \vec{a} \cdot \vec{\sigma},$$

where I and $\vec{\sigma}$ are the 2×2 identity and Pauli matrices. The invariant measure is given by

$$\begin{aligned} \int d\mu_{SU(2)} &= \int d^4 a \delta(a^2 - 1) \\ &= \int da_0 d|\vec{a}| d^3 \hat{n} |\vec{a}|^2 \delta(a_0^2 + \vec{a}^2 - 1) \\ &\propto \int da_0 \sqrt{1 - a_0^2}. \end{aligned}$$

The last line assumes a uniform distribution of $d^3\hat{n}$. We see that a_0 plays the role of $\ell = \cos(q_1)$: The change of coordinates from ℓ to q_1 gives an extra factor of the square root term, leading to the same expression of the invariant measure in Eq. (25).

B. $N_c = 3$

For the SU(3) gauge group there are two independent eigenphases $\vec{q} = (q_1, q_2, -q_1 - q_2)$; hence

$$\hat{\ell}_F = \text{diag}(e^{iq_1}, e^{iq_2}, e^{-i(q_1+q_2)}), \quad (26)$$

and the order parameter field is

$$\begin{aligned} \ell &= X + iY, \\ X &= \frac{1}{3}(\cos q_1 + \cos q_2 + \cos(q_1 + q_2)), \\ Y &= \frac{1}{3}(\sin q_1 + \sin q_2 - \sin(q_1 + q_2)). \end{aligned}$$

The adjoint angles are shown in Table I. Using these with Eq. (20) the invariant measure can be computed

$$\begin{aligned} H(q_1, q_2) &= 64 \sin^2 \frac{(q_1 - q_2)}{2} \\ &\times \sin^2 \frac{(2q_1 + q_2)}{2} \sin^2 \frac{(q_1 + 2q_2)}{2}. \end{aligned} \quad (27)$$

We can also express the result in terms of the Cartan parameters. The two independent directions can be chosen to be

$$\begin{aligned} \vec{v}_1 &= (1, 0, -1), \\ \vec{v}_2 &= (1/2, -1, 1/2); \end{aligned} \quad (28)$$

$$\begin{aligned} \gamma_1 &= q_1 + q_2/2, \\ \gamma_2 &= -q_2 \end{aligned} \quad (29)$$

can be taken as independent variables; and the invariant measure reads

TABLE I. Adjoint angles of the Polyakov loop operator for the SU(3) group.

Q_1	Q_2	
0	0	
$Q_3 = -Q_6$	$Q_4 = -Q_7$	$Q_5 = -Q_8$
$q_1 - q_2$	$2q_1 + q_2$	$q_1 + 2q_2$

$$\begin{aligned} H(\gamma_1, \gamma_2) &\propto \sin^2 \frac{(\gamma_1 - 3/2\gamma_2)}{2} \\ &\times \sin^2 \gamma_1 \sin^2 \frac{(\gamma_1 + 3/2\gamma_2)}{2}. \end{aligned} \quad (30)$$

Specific to the SU(3) gauge group, the two independent degrees of freedom can be identified with the trace of the Polyakov loop operator in the fundamental representation ℓ , and the invariant measure can be expressed via X, Y :

$$\begin{aligned} H(X, Y) &= 27 \times (1 - 6(X^2 + Y^2) \\ &+ 8(X^3 - 3XY^2) - 3(X^2 + Y^2)^2). \end{aligned} \quad (31)$$

For $N_c > 3$, the invariant measure generally depends on $N_c - 1$ independent angles, and therefore is not expressible solely in terms of (X, Y) .

C. $N_c = 4$

The analysis for $N_c = 4$ and beyond proceeds in a similar fashion. For the SU(4) gauge group there are three independent eigenphases:

$$\vec{q} = (q_1, q_2, q_3, q_4) \quad (32)$$

with $q_4 = -(q_1 + q_2 + q_3)$.

The order parameter field is given by

$$\begin{aligned} \ell &= X + iY, \\ X &= \frac{1}{4}(\cos q_1 + \cos q_2 + \cos q_3 + \cos(q_1 + q_2 + q_3)), \\ Y &= \frac{1}{4}(\sin q_1 + \sin q_2 + \sin q_3 - \sin(q_1 + q_2 + q_3)). \end{aligned} \quad (33)$$

The $15 = 3 + 6 + 6$ adjoint angles are composed of three zeros, six nontrivial angles, and their negative values (see Table II).

The invariant measure can be constructed from the nontrivial adjoint angles:

$$H(\vec{q}) \propto \prod_{j=4-9} \sin^2 Q_j. \quad (34)$$

To translate this into the Cartan $\vec{\gamma}$, we can use the following basis vectors:

$$\begin{aligned} \vec{v}_1 &= (1, 1/3, -1/3, -1), \\ \vec{v}_2 &= (1, -1, -1, 1), \\ \vec{v}_3 &= (1/3, -1, 1, -1/3). \end{aligned} \quad (35)$$

In particular, going along \vec{v}_1 , corresponding to the uniform eigenvalue ansatz [13], the order parameter field is purely real, and through γ_1 we can relate the invariant measure to the Polyakov loop:

TABLE II. Adjoint angles of the Polyakov loop operator for the $SU(4)$ group.

Q_1	Q_2	Q_3
0	0	0
$Q_4 = -Q_{10}$ $q_1 - q_2$	$Q_5 = -Q_{11}$ $q_1 - q_3$	$Q_6 = -Q_{12}$ $q_2 - q_3$
$Q_7 = -Q_{13}$ $2q_1 + q_2 + q_3$	$Q_8 = -Q_{14}$ $q_1 + 2q_2 + q_3$	$Q_9 = -Q_{15}$ $q_1 + q_2 + 2q_3$

$$\begin{aligned}
 X &= \frac{1}{2}(\cos \gamma_1 + \cos(\gamma_1/3)), \\
 Y &= 0,
 \end{aligned} \tag{36}$$

and

$$H(\vec{q} \rightarrow \gamma_1 \vec{v}_1) \propto \sin^6(\gamma_1/3) \sin^4(2\gamma_1/3) \sin^2(\gamma_1), \tag{37}$$

compared to a similar projection in the $SU(3)$ case

$$H(\vec{q} \rightarrow \gamma_1 \vec{v}_1) \propto \sin^2 \frac{\gamma_1}{2} \sin^2 \gamma_1 \sin^2 \frac{\gamma_1}{2}. \tag{38}$$

III. POLYAKOV LOOP AND THE SUSCEPTIBILITIES

A. General results

Once an effective potential is specified, its minimization and the extraction of various observables are standard procedure [14]. Here we simply display the results in Fig. 1 and highlight some observations:

- (i) First, the order of the phase transition naturally changes from second order for $N_c = 2$ to first order for $N_c \geq 3$. Note that the same set of model parameters has been used in the calculations.
- (ii) Second, the two susceptibilities derived for $N_c \geq 3$ are equal in the confined phase, and a narrow aspect ratio for the shape of the potential, i.e., $\chi_T \ll \chi_L$ in the deconfined phase. This case is known for $N_c = 3$ [24]. Equation (6) makes it possible to study the fluctuations beyond $N_c = 3$, and for the first time we can verify a similar trend is observed in this class of model for $N_c \geq 4$ under the uniform eigenvalue ansatz [13].
- (iii) It is expected that the first order phase transition becomes stronger as N_c increases. This is the case in this model, and comparing the $N_c = 4$ case with $N_c = 3$, we observe the Polyakov loop at T_d increases, while the magnitudes of the susceptibilities decrease. The latter suggests larger curvatures of the potential around the minima, which sets the stage for a stronger phase transition. As N_c increases

further, we find that $\ell(T_d)$ tends to ≈ 0.5 , while the decreasing trend of the susceptibilities continues.²

The Landau parameters can be directly extracted in this model. For the case of $SU(3)$ along the real line, we write

$$\frac{U}{T^4} = \bar{u}_0 + \bar{u}_2 X^2 + \bar{u}_3 X^3 + \bar{u}_4 X^4 + \dots \tag{39}$$

Expanding potentials (12) and (13) in powers of X , we obtain (in the Boltzmann limit)

$$\begin{aligned}
 \bar{u}_0 &= \frac{1}{\pi^2} \left(\frac{m_A}{T} \right)^2 K_2 \left(\frac{m_A}{T} \right), \\
 \bar{u}_2 &= \frac{3b}{T^3} - \frac{9}{\pi^2} \left(\frac{m_A}{T} \right)^2 K_2 \left(\frac{m_A}{T} \right), \\
 \bar{u}_3 &= -\frac{4b}{T^3} + \frac{27}{\pi^2} \left(\frac{m_A}{T} \right)^2 K_2 \left(\frac{2m_A}{T} \right), \\
 \bar{u}_4 &= \frac{21b}{2T^3} - \frac{81}{4\pi^2} \left(\frac{m_A}{T} \right)^2 K_2 \left(\frac{2m_A}{T} \right),
 \end{aligned} \tag{40}$$

where K_2 is the modified Bessel function of the second kind (order 2). These relations link the Landau parameters to properties of the underlying gluons. To derive these results we have used the fact that

$$\begin{aligned}
 \text{Tr} \hat{\mathcal{L}}_A &= (\text{Tr} \hat{\mathcal{L}}_F)^2 - 1 \\
 &\xrightarrow{SU(3)} 9X^2 - 1, \\
 \text{Tr} \hat{\mathcal{L}}_A^2 &= (\text{Tr} \hat{\mathcal{L}}_F^2)^2 - 1 \\
 &\xrightarrow{SU(3)} 36X^2 - 108X^3 + 81X^4 - 1
 \end{aligned} \tag{41}$$

along the real line. The expansion works best in the confined phase, where $X \ll 1$. Note that the cubic term arises naturally from $\text{Tr} \hat{\mathcal{L}}_A^2$, and we can readily verify the standard scenario of a first order phase transition: $\bar{u}_3 < 0$, $\bar{u}_4 > 0$, and \bar{u}_2 changes sign (from positive to negative) close to T_d . See Fig. 2. The susceptibilities can be simply constructed from

$$(T^3 \chi_{L,T})^{-1} \approx (2\bar{u}_2). \tag{42}$$

Thus, the observables are driven by a competition between the confining and the deconfining potentials. This is a general observation for the class of models we study. Also the condition

$$\bar{u}_2(T) = 0 \tag{43}$$

is useful for a qualitative understanding of T_d , giving $T \approx 0.29$ GeV instead of the true value $T_d = 0.274$ GeV, calculated numerically.

²The value becomes $\ell(T_d, N_c \rightarrow \infty) \approx 0.6$ for models B and C introduced later. See Eq. (83).

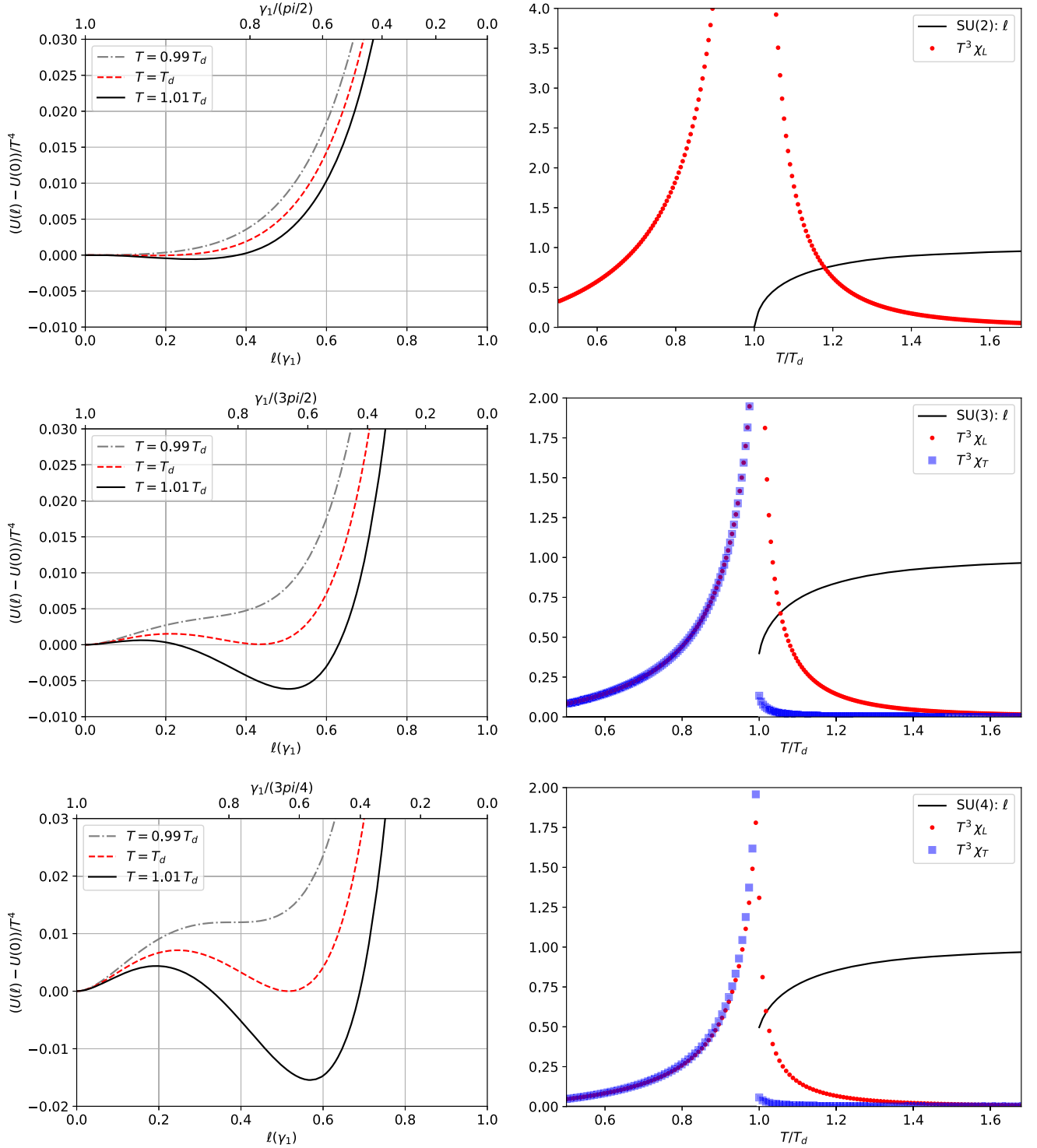


FIG. 1. The Polyakov loop potentials (11) (left) and the derived observables: the Polyakov loop expectation values, the longitudinal and the transverse susceptibilities (right) for $N_c = 2, 3, 4$.

B. Gluon density in the presence of Polyakov loop

A key feature of an effective Polyakov loop model is a description of the thermal densities of gluons and quarks in the presence of a Polyakov loop mean field. These can be conveniently expressed in terms of the eigenphases. Take,

for example, the case for SU(3), along the real line, they depend only on a single angle variable γ_1 (i.e., $\gamma_2 = 0$),

$$\hat{\mathcal{L}}_F \rightarrow \text{diag}(e^{i\gamma_1}, 1, e^{-i\gamma_1}) \quad (44)$$

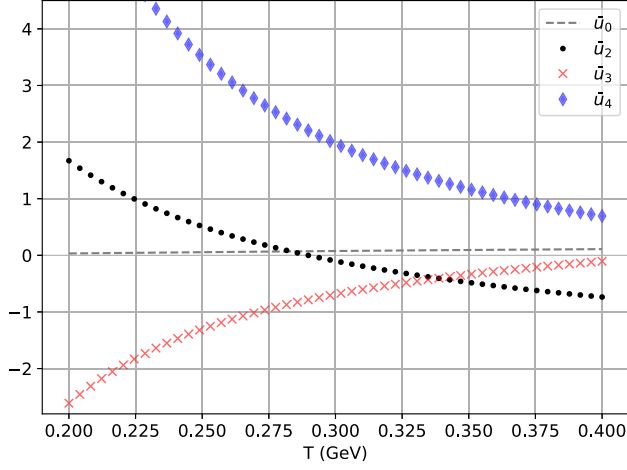


FIG. 2. Landau parameters [Eq. (40)] derived from the effective potential (11) as functions of temperature.

and

$$\hat{\mathcal{L}}_A \rightarrow \text{diag}(1, 1, e^{i\gamma_1}, e^{2i\gamma_1}, e^{i\gamma_1}, e^{-i\gamma_1}, e^{-2i\gamma_1}, e^{-i\gamma_1}), \quad (45)$$

such that

$$n_{\text{glue}}(\gamma_1) = \int \frac{d^3k}{(2\pi)^3} \sum_{i=1-8} \frac{\hat{\mathcal{L}}_A^{(j)}}{e^{\beta E_A} - \hat{\mathcal{L}}_A^{(j)}}. \quad (46)$$

Note that as $\gamma_1 \rightarrow 0$, $\hat{\mathcal{L}}_A$ becomes an identity in the 8×8 adjoint space, and Eq. (46) recovers the free quantum Bose gas limit,

$$n_{\text{glue}}(\gamma_1 \rightarrow 0) = 8 \times \int \frac{d^3k}{(2\pi)^3} \frac{1}{e^{\beta E_A(k)} - 1}. \quad (47)$$

An analogous expression can be derived for quarks, except that the trace is over the entries of the Polyakov loop operator in the fundamental representation $\hat{\mathcal{L}}_F$. It can also be expressed as a function of γ_1 :

$$n_{\text{quarks}}(\gamma_1) = \int \frac{d^3k}{(2\pi)^3} \sum_{i=1-3} \frac{\hat{\mathcal{L}}_F^{(j)}}{e^{\beta E_Q(k)} + \hat{\mathcal{L}}_F^{(j)}}. \quad (48)$$

Similarly the free quantum fermion gas limit is recovered at $\gamma_1 \rightarrow 0$,

$$n_{\text{quarks}}(\gamma_1 \rightarrow 0) = 3 \times \int \frac{d^3k}{(2\pi)^3} \frac{1}{e^{\beta E_Q(k)} + 1}. \quad (49)$$

A plot of these thermal densities are shown in Fig. 3, illustrated for the case of $N_c = 2, 3, 4$. Note that the x axis is the corresponding traced Polyakov loops, projected along the real line:

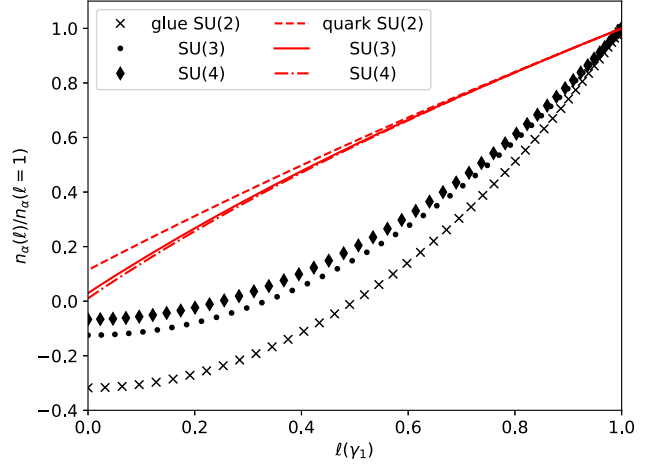


FIG. 3. Thermal densities of quarks and gluons in the presence of a background Polyakov loop field for $N_c = 2, 3, 4$. The results are evaluated at $T = 0.24$ GeV with an effective gluon mass $m_A = 0.756$ GeV and a quark mass $m_Q = 0.1$ GeV.

$$\ell_{\text{SU}(2)}(\gamma_1) = \cos \gamma_1,$$

$$\ell_{\text{SU}(3)}(\gamma_1) = \frac{1}{3}(1 + 2 \cos \gamma_1),$$

$$\ell_{\text{SU}(4)}(\gamma_1) = \frac{1}{2}(\cos \gamma_1 + \cos(\gamma_1/3)). \quad (50)$$

An important observation is that both densities are substantially suppressed at $\ell \rightarrow 0$ compared to the free gas limits $\ell \rightarrow 1$. This is how confinement is represented in this class of models: a statistical confinement that relates the thermal abundances of quarks and gluons to the expectation value of the $Z(N_c)$ order parameter, i.e., the Polyakov loop.

For gluons, the $\ell = 0$ limit turns mildly negative. This does not necessarily mean we have a negative pressure in the bulk, since other contributions, such as those coming from the confining ghosts, can reverse this negative value. The thermal distribution of confining gluons in the QCD medium is still an open issue, and a small negative value in some momentum range is not ruled out. Nevertheless, it is likely that the beyond one-loop, nonperturbative interactions will produce further corrections to this quantity.³ A similar plot from a nonperturbative study, such as Schwinger Dyson equations in a given gauge, can help to clarify the issue [35–42].

In any case the suppression discussed here, linked to an order parameter for the spontaneous $Z(N_c)$ breaking, is an

³The standard prescription in an effective model is to simply subtract the potential at $\ell = 0$. This fixes the problem of negative partial pressure and density of gluons in the confined phase. Of course, results for the Polyakov loops and their fluctuations are not affected. However, one then needs to correct for the right number of gluonic degrees of freedom in the deconfined phase at high temperatures.

effective description. There are interesting differences from models which predict the suppression in the spectrum via an infrared divergent mass (and wave function) renormalizations [43]. The task remains to understand the connections between various models of confinement, and to further explore the dynamical aspects of confining quasi-gluons in the QCD medium, practical for building phenomenology of the thermal system of glueballs and other objects.

IV. CURVATURE MASSES OF CARTAN ANGLES

A. Gauge dependence and effects of wave function renormalization

In Ref. [15] the phase transition of the pure Yang-Mills system is studied using the background field method in the Landau-DeWitt gauge. A confining potential is motivated from the ghost determinant:

$$\text{Tr} \ln \bar{D}_{\text{adj}}^2. \quad (51)$$

This gives a potential of exactly the same form as U_{glue} in Eq. (13), but with an opposite sign, and is hence $Z(N_c)$ restoring. Note that the correct way to account for a ghost contribution to the thermodynamic potential involves a bosonic Matsubara sum of the relevant operator (with a factor of -1), instead of a fermionic Matsubara sum [44]. The total potential can be written as

$$U_{\text{tot}} = 3U_1(m_A) - U_1(0). \quad (52)$$

This form makes it obvious that we are considering three gluons and one ghost. Both terms can be expressed with U_1 that reads

$$\begin{aligned} U_1(m_A) &= \frac{1}{2\beta} \sum_a \int \ln(\tilde{k}_a^2 + m_A^2) \\ &= T \int \frac{d^3k}{(2\pi)^3} \text{Tr}_A \ln(I - \hat{\ell}_A e^{-\beta E_A(k)}) \end{aligned} \quad (53)$$

with

$$\tilde{k}_a^2 = \left(\omega_n + \frac{Q_a}{\beta} \right)^2 + (\vec{k})^2. \quad (54)$$

Note that the invariant measure term (20) can be regarded as a limiting case of U_1 with $E_A \rightarrow 0$.⁴ One can speculate the form of potential in the 't Hooft-Feynman gauge to read

⁴In the axial gauge [33], it was argued the invariant measure term is canceled by a similar term in the glue potential. The case of massive gluons remains to be explored.

$$\begin{aligned} U_{\text{tot}} &= 2U_1(m_A) + \Delta U_\xi, \\ \Delta U_\xi &= (1 + \Delta n_\xi) \times (U_1(m_A) - U_1(0)). \end{aligned} \quad (55)$$

The subscript ξ signifies the possible gauge dependence, e.g., $\Delta n_\xi = 0(1)$ in Landau-DeWitt ('t Hooft-Feynman) gauge. Note that the gluon mass m_A itself can depend on the gauge choice. Nevertheless, in all cases the physical limit of 2 gluonic degrees of freedom at high temperature (the Stefan-Boltzmann limit) is recovered when we set $m_A = 0$, $\hat{\ell}_A = I$ in the perturbative vacuum.

We next expand the model to include effects of wave function renormalizations of gluons and ghosts [23]. Assuming the background field continues to enter as Eq. (54), e.g., when the ghost propagator is modified by

$$\frac{1}{\tilde{k}^2} \rightarrow \frac{Z_{\text{gh}}(\tilde{k}^2)}{\tilde{k}^2}, \quad (56)$$

the corresponding change in the potential reads

$$\text{Tr} \ln \tilde{k}^2 \rightarrow \text{Tr}(\ln \tilde{k}^2 - \ln Z_{\text{gh}}(\tilde{k}^2)). \quad (57)$$

A further simplification is possible if we approximate Z_{gh} in the Gribov-Stingl form [23]:

$$Z_{\text{gh}} \propto \left(\frac{\tilde{k}^2 + R_1^2}{\tilde{k}^2 + R_2^2} \right) \quad (58)$$

with some mass scales $R_{1,2}$. Note that $Z_{\text{gh}}(\tilde{k}^2 \rightarrow \infty) \rightarrow 1$. The corresponding modification in the effective Polyakov loop potential is given by

$$U_1(0) \rightarrow U_1(0) - (U_1(R_1) - U_1(R_2)) \quad (59)$$

for each ghost field. For demonstration, we fit the result of the lattice determination of the wave function renormalization of the ghost propagator [45] (in Landau gauge) with the parametrization (58). A reasonable fit is obtained with parameters $R_1 = 1.335$ GeV and $R_2 = 0.732$ GeV. A similar scheme can be applied to the gluons, with a slightly modified form:

$$\begin{aligned} Z_{\text{glue}} &= \left(\frac{\tilde{k}^2 + R_1^2}{\tilde{k}^2 + R_2^2} \right)^{g_1} \left(\frac{\tilde{k}^2 + R_3^2}{\tilde{k}^2 + R_4^2} \right)^{g_2}, \\ D_{\text{glue}} &= \frac{Z_{\text{glue}}}{\tilde{k}^2 + m_A^2}. \end{aligned} \quad (60)$$

The parameters are $(g_1, R_1, R_2) = (4, 2.615, 1.660)$, $(g_2, R_3, R_4) = (1, 2.616, 6.794)$, and $m_A = 0.756$, all in appropriate units of GeVs. The results are shown in Fig. 4.

The change in the effective potential can be intuitively understood as follows: The enhancement of Z_{gh} at low momenta dictates $R_1 > R_2$, with a stronger Boltzmann suppression gives $|U_1(R_1)| < |U_1(R_2)|$, and finally leads to a strengthening of the ghost potential (while preserving its

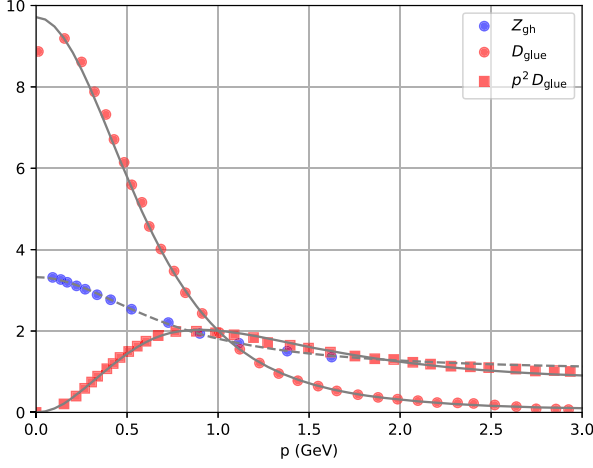


FIG. 4. Fits of ($T = 0$) LQCD results [45] of gluon propagator and ghost wave function renormalization with the generalized Gribov-Stingl form in Eqs. (58) and (60).

sign). See Eq. (59).⁵ A stronger potential is also found when implementing the lattice result of the gluon propagator with a wave function renormalization. On the other hand, the value of T_d depends on the competition between the two and requires an actual calculation to deduce the trend.

We thus obtain a unified framework to discuss the modeling of an effective potential in different approximation schemes:

$$U_{\text{tot}} = 2U_1(m_A) + \Delta U_\xi \quad (61)$$

with

$$\Delta U_\xi = (1 + \Delta n_\xi)(U_1(m_A) - U_1(0)) + \sum_j g_j (U_1(R_1^{(j)}) - U_1(R_2^{(j)})). \quad (62)$$

The key observation is that the same group structure appears in various contributions to the potential, and details of gluon and ghost propagators are subsumed into the model parameters. The effective framework thus provides a transparent way to link the Polyakov loop observables with those of the gauge-fixed correlators [37,42].

In the following, we investigate how different model assumptions of the gauge-fixed correlators affect the fluctuations of the Polyakov loop.

⁵It is also possible that the function drops rapidly to zero in the deep infrared, and hence the form (59) needs to be modified [37,46–49]. Furthermore, there are more refined studies on decomposing the gluon propagators into $Z_{\text{glue}}(k)$ and mass function $m_A(k)$ [50,51]. The scenario in other gauges, and the efficacy of the commonly used approximation schemes, such as static approximation or expansions around simple poles, should be investigated in the future.

B. Susceptibilities and masses of Cartan angles

We choose to focus on the physical case of $N_c = 3$. This case is unique in the sense that the two Cartan angles $\gamma_{1,2}$ can be directly identified with the two degrees of freedom of the Polyakov loop, i.e., X, Y . The (2×2) Jacobian matrix allows the translation between $(\gamma_1, \gamma_2) \leftrightarrow (X, Y)$:

$$J = \frac{\partial\{X, Y\}}{\partial\{\gamma_1, \gamma_2\}},$$

$$J_{11} = \frac{1}{3} \left(-\sin \frac{2\gamma_1 + \gamma_2}{2} - \sin \frac{2\gamma_1 - \gamma_2}{2} \right),$$

$$J_{12} = \frac{1}{3} \left(-\frac{1}{2} \sin \frac{2\gamma_1 + \gamma_2}{2} + \frac{1}{2} \sin \frac{2\gamma_1 - \gamma_2}{2} - \sin \gamma_2 \right),$$

$$J_{21} = \frac{1}{3} \left(\cos \frac{2\gamma_1 + \gamma_2}{2} - \cos \frac{2\gamma_1 - \gamma_2}{2} \right),$$

$$J_{22} = \frac{1}{3} \left(-\frac{1}{2} \cos \frac{2\gamma_1 + \gamma_2}{2} + \frac{1}{2} \cos \frac{2\gamma_1 - \gamma_2}{2} - \cos \gamma_2 \right). \quad (63)$$

We stress that studying the order parameter and its fluctuations along two independent directions is mandated by the existence of two independent Cartan generators, both relevant to describing the gauge group $SU(3)$. Many existing works have neglected the imaginary direction in the potential, and hence the appropriate field derivatives cannot be performed.

We define the (dimensionless) curvature mass tensor for the Cartan angles as [52]

$$\bar{m}_{ij}^2 = \frac{\partial^2 U(\gamma_1, \gamma_2)}{\partial \gamma_i \partial \gamma_j} \frac{1}{T^4}. \quad (64)$$

The tensor elements are to be evaluated with values of γ_1 which minimize the potential, and $\gamma_2 \rightarrow 0$. For the class of potentials considered the off-diagonal terms vanish. The relation to the curvature masses associated with the (X, Y) fields [53] is thus

$$\bar{m}_{11}^2 = J_{11}^2 \bar{m}_{XX}^2 + J_{21}^2 \bar{m}_{YY}^2,$$

$$\bar{m}_{22}^2 = J_{12}^2 \bar{m}_{XX}^2 + J_{22}^2 \bar{m}_{YY}^2, \quad (65)$$

where

$$\bar{m}_{XX}^2 = \frac{\partial^2 U}{\partial X \partial X} \frac{1}{T^4},$$

$$\bar{m}_{YY}^2 = \frac{\partial^2 U}{\partial Y \partial Y} \frac{1}{T^4}. \quad (66)$$

A further simplification comes from the fact that the Jacobian matrix, evaluated along the real line (arbitrary $\gamma_1, \gamma_2 = 0$), is also diagonal:

$$\begin{aligned}
J_{11} &= -\frac{2}{3}\sin\gamma_1 = -\frac{1}{\sqrt{3}}\sqrt{(1-\ell)(1+3\ell)}, \\
J_{22} &= -\frac{2}{3}\left(\sin\frac{\gamma_1}{2}\right)^2 = -\frac{1}{2}(1-\ell), \\
J_{12} &= 0, \\
J_{21} &= 0,
\end{aligned} \tag{67}$$

where $\ell = \frac{1}{3}(1 + 2\cos\gamma_1)$. Note that in the confined phase $\gamma_1 \rightarrow 2\pi/3$,

$$\begin{aligned}
J_{11} &\rightarrow -1/\sqrt{3}, \\
J_{22} &\rightarrow -1/2,
\end{aligned} \tag{68}$$

and in the deconfined phase $\gamma_1 \rightarrow 0$ they vanish as

$$\begin{aligned}
J_{11} &\rightarrow -\frac{2}{\sqrt{3}}\sqrt{(1-\ell)}, \\
J_{22} &\rightarrow -\frac{1}{2}(1-\ell),
\end{aligned} \tag{69}$$

with $\ell \rightarrow 1$. Note that $|J_{22}| \ll |J_{11}|$ in this limit. We thus obtain the following relation between the curvature masses of Cartan angles and the Polyakov loop susceptibilities:

$$\begin{aligned}
\bar{m}_{11}^2 &= \frac{4}{9}(\sin\gamma_1)^2\bar{m}_{\chi X}^2, \\
\bar{m}_{22}^2 &= \frac{4}{9}\left(\sin\frac{\gamma_1}{2}\right)^4\bar{m}_{\chi Y}^2,
\end{aligned} \tag{70}$$

with the Polyakov loop susceptibilities identified as

$$\begin{aligned}
(T^3\chi_L) &= \frac{1}{\bar{m}_{\chi X}^2} = \frac{(1-\ell)(1+3\ell)}{3\bar{m}_{11}^2}, \\
(T^3\chi_T) &= \frac{1}{\bar{m}_{\chi Y}^2} = \frac{(1-\ell)^2}{4\bar{m}_{22}^2}.
\end{aligned} \tag{71}$$

This is a useful relation linking the Polyakov loop observables to those based on the Cartan angles. The latter can eventually be linked to A_0 and the transverse gluons. Note that such a clean separation of contributions to $T^3\chi_{L,T}$ from \bar{m}_{ii}^2 is only true for $N_c = 3$. Each susceptibility generally receives contributions from all Cartan curvature masses \bar{m}_{ii}^2 .

We derive an analytic expression for these Cartan curvature masses at ultrahigh temperatures. The effective potential is expected to approach

$$U(\gamma_1, \gamma_2) \approx 2U_1(m_A = 0). \tag{72}$$

Using the exact result of the integral

$$\begin{aligned}
U_a(Q_a) &= T \int \frac{d^3k}{(2\pi)^3} \ln(I - e^{iQ_a} e^{-\beta k}) \\
&= -\frac{T^4}{\pi^2} \text{PolyLog}(4, e^{iQ_a}),
\end{aligned} \tag{73}$$

and the polynomial expansion of the PolyLog function (valid in the restricted range of $Q_a \in [0, \pi]$)

$$\frac{U_a(Q_a) + U_a(-Q_a)}{T^4} = -\frac{\pi^2}{45} + \frac{Q_a^2}{6} - \frac{Q_a^3}{6\pi} + \frac{Q_a^4}{24\pi^2}, \tag{74}$$

we obtain the potential [see Table I and Eq. (29)]

$$\begin{aligned}
\frac{U(\gamma_1, \gamma_2)}{T^4} &\approx -\frac{16\pi^2}{90} + 2\gamma_1^2 + \frac{3}{2}\gamma_2^2 \\
&\quad + \frac{3(4\gamma_1^2 + 3\gamma_2^2)^2}{32\pi^2} - \frac{20\gamma_1^3 + 27\gamma_1\gamma_2^2}{6\pi}.
\end{aligned} \tag{75}$$

The curvature masses (64) can be readily deduced:

$$\begin{aligned}
\bar{m}_{11}^2 &\rightarrow 4, \\
\bar{m}_{22}^2 &\rightarrow 3.
\end{aligned} \tag{76}$$

It follows from Eq. (71) that while both susceptibilities approach zero at high temperatures, with $\chi_T \ll \chi_L$, one can extract a finite limit for the curvature masses. Note that if we take

$$\gamma_{1,2} \rightarrow r_{1,2}\beta g A_4, \tag{77}$$

these curvature masses are related to the dimensionful m_{A_4} via

$$\begin{aligned}
\bar{m}_{ii}^2 &= \frac{m_{A_4}^2}{g^2 T^2 r_i^2}, \\
m_{A_4}^2 &= \frac{\partial^2 U}{\partial A_4 \partial A_4}
\end{aligned} \tag{78}$$

for $i = 1, 2$. The fact that \bar{m}_{ii}^2 has a finite limit forces

$$m_{A_4} \propto gT, \tag{79}$$

as expected for a Debye screening mass. We stress that m_{A_4} should be distinguished from the effective gluon mass m_A introduced. The latter captures the infrared enhancement originated from the nonperturbative vacuum and exists even at vanishing temperature.

The behaviors of these curvature masses at low temperatures are lesser known. In the confined phase, $Z(3)$ symmetry requires [24], in addition to $\langle \hat{\mathcal{L}}_F \rangle = 0$,

$$\begin{aligned}
\langle \hat{\mathcal{L}}_F^2 \rangle &= 0 \\
\Rightarrow \langle (X^2 - Y^2) \rangle &= 0.
\end{aligned} \tag{80}$$

This means the two susceptibilities are equal in this phase. It follows from Eq. (71) that

$$\frac{\bar{m}_{22}^2}{\bar{m}_{11}^2} = \frac{3}{4} \tag{81}$$

in the confined phase. Note that the same ratio is observed in the high temperature limit (76).

Other than the constraint (81) on the ratio, there is no restriction from symmetry concerning their magnitudes. In the language of an effective model, they reflect a competition between the confining (ghost) and the deconfining (glue) parts of the potential. And unlike $\langle \hat{\mathcal{L}}_F \rangle$, they are finite and temperature dependent even in the confined phase.

To examine how the curvature masses associated with the Cartan angles depend on the assumed properties of the gluons and ghosts, we compute the observables in the following arrangements of the effective potential:

- (i) model A: an invariant measure term (12) with two transverse gluons:

$$U = -\frac{1}{2}b \ln H + 2U_1(m_A). \quad (82)$$

- (ii) model B: a ghost field term and three transverse gluons:

$$U = -U_1(m_A = 0) + 3U_1(m_A). \quad (83)$$

- (iii) model C: model B implemented with wave function renormalization effects discussed.

With no further tuning of model parameters, we obtain $T_d \approx (0.274, 0.274, 0.27)$ GeV for models A, B, and C. The results of Cartan masses are shown in Fig. 5.

We first report that Eq. (71) works: i.e., the same results of the susceptibilities are obtained when the curvature tensor [Eq. (8)] is directly constructed by taking the appropriate (X, Y) -field derivatives on the potential derived in Ref. [22]. This gives some confidence for the general applicability of Eq. (6) for the general N_c problem.

The most obvious feature of the curvature masses is the dip around T_d . Note that a very similar behavior is found for the A_0 -gluon screening mass extracted from LQCD when studying the inverse of the longitudinal propagator [54]. See also the discussion in Ref. [55]. In the effective model, this follows from the relation to the Polyakov loop susceptibilities. While the gluon (and ghost) parameters employed are smooth, the discontinuity is inherited from minimizing the mean-field potential. Note that a strong temperature dependence of these observables naturally arises without the need of introducing temperature dependent model parameters. In fact, in an improved scheme, the model parameters, including the additional temperature dependence, should be determined self-consistently.

The high temperature limits (76) are approached very gradually: at $T \approx 30T_d$ and from above (below) for models A, C (B). Note that model B has a known issue in the deconfined phase that the Polyakov loop reaches unity too rapidly and the model may not be reliable beyond this point. Apparently, the existence of a secondary dip in the curvature masses in model B (also in model C) also comes

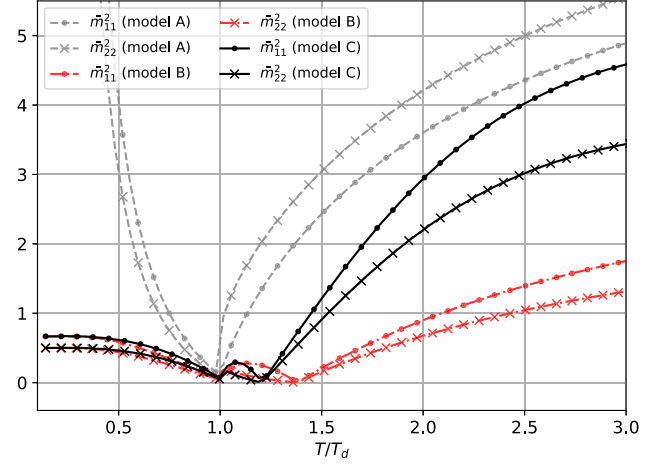


FIG. 5. Curvature masses associated with the Cartan angles calculated for different models (see text).

with this problem. This does not happen to Model A, where the invariant measure term prevents this problematic behavior. It has been suggested that a two-loop calculation may remove this artifact [56]. It would be interesting to see the corresponding modification in the curvature masses.

There is no strict theoretical constraint on the low temperature behaviors of these curvature masses. The constraint (81) on their ratio is verified in all cases. What is clear from the effective model study is that they depend strongly on the choice of the confining potential. This is particularly obvious in the $T \rightarrow 0$ limit: In model A, they diverge as [see Eqs. (40) and (70)]

$$\begin{aligned} \bar{m}_{11}^2 &\rightarrow \frac{2b}{T^3}, \\ \bar{m}_{22}^2 &\rightarrow \frac{3b}{2T^3}. \end{aligned} \quad (84)$$

In model B we get instead the finite results:

$$\begin{aligned} \bar{m}_{11}^2 &\rightarrow \frac{2}{3}, \\ \bar{m}_{22}^2 &\rightarrow \frac{1}{2}. \end{aligned} \quad (85)$$

The effect of wave function renormalization (model C), with the parameters chosen, is found to be small at low temperatures, but becomes substantial close to and above T_d .

If we insist on imposing the matching condition (78) and identify the A_0 -gluon screening mass with m_A , we would obtain a $\propto \frac{1}{T^2}$ behavior for these curvature masses. It would thus be interesting to examine these observables with other gauge choices [57,58]: to see whether the differences are due to gauge artifacts, and to gain insights in reliably describing the low temperature behavior of the Polyakov loop potential.

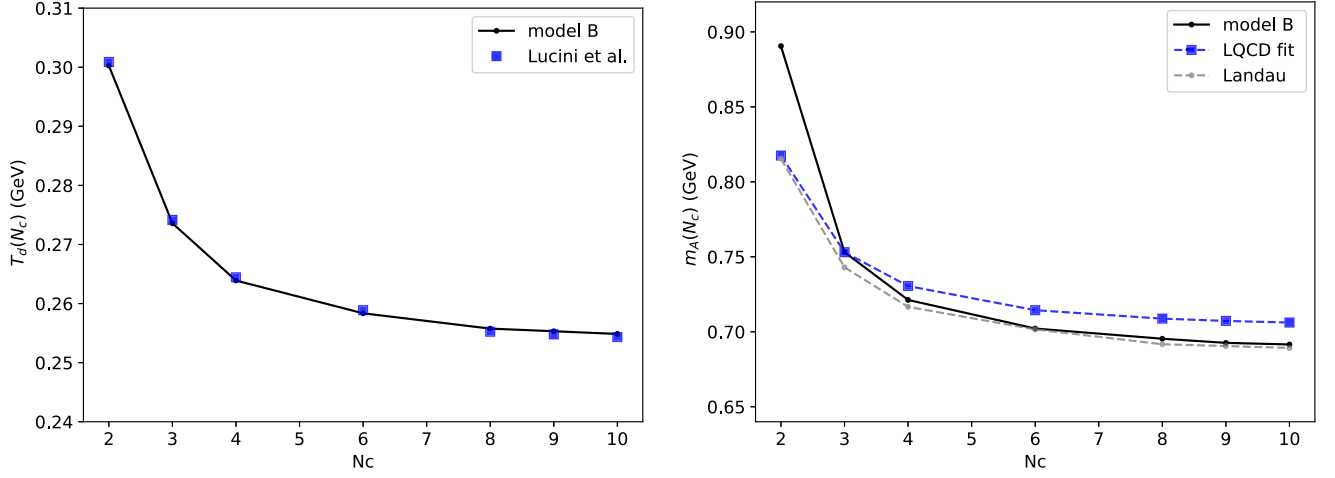


FIG. 6. The critical temperatures T_d of model B (83) (left) using the input masses $m_A(N_c)$ indicated in the right panel. The latter are adjusted to fit the LQCD results on $T_d(N_c)$ [61] and are compared to a fit to the LQCD of (half the) 0^{++} glueball mass [62]. The gray dashed line shows the result based on Landau parameter analysis (88) (\bar{u}_2).

C. The appearance of glueballs

Finally we speculate how the glueballs may enter the effective description. In the current model a phenomenological gluon mass m_A is introduced, which serves to suppress the gluon contribution (deconfining) in the potential at low temperatures. This also sets the scale for the critical temperature T_d .

In Refs. [29,59], a robust theoretical framework to introducing quasigluonic excitation is proposed via a constituent Fock space expansion. There, a nontrivial QCD vacuum, as in the Bardeen-Cooper-Schrieffer (BCS) theory, is postulated, and with a Bogoliubov-Valatin transformation the (massive) quasigluons are derived from the effective one-body Hamiltonian. This mirrors the one-loop gluon potential considered here.

In addition, glueball spectra can be derived with the same Hamiltonian using the two-gluon states built from these quasigluons. A key observation is that the lowest lying states receive most of their masses from the quasigluons, i.e.,

$$m_{\text{GB}} \approx 2m_A, \quad (86)$$

e.g., $m_{\text{GB}} \approx 1.7(2.1)$ GeV for the lowest $0^{++}(0^{+-})$ state, with $m_A = 0.8$ GeV in Ref. [29]. This naturally suggests a constituent model for the glueball states. Neglecting their interactions with the Polyakov loops, we may consider free gas of glueballs as an approximation for the $2 \rightarrow 2$ contribution to the partition function.⁶ See Ref. [60] for an elaborate treatment of thermal glueballs.

A nontrivial relation suggested by the effective model is a link between $T_d(N_c)$ and $m_A(N_c)$. Model B is ideal for

⁶This is similar to the case where a σ -meson is generated in an Nambu–Jona-Lasinio model and approximating its partial thermal pressure by a free Bose gas of mass $m_\sigma \approx 2M_Q$.

this illustration as m_A is the only adjustable parameter of the model. Tuning m_A to match the model T_d with the LQCD results [61] for various N_c 's, we extract the expected N_c dependence of m_A . See Fig. 6.

The $m_A(N_c)$'s show a similar trend exhibited by a fit to LQCD 0^{++} glueball masses [62]. The fit employs the functional form

$$m_{\text{GB}}^{\text{LQCD}}(N_c)/\sqrt{\sigma} \approx m_\infty + c/N_c^2 \quad (87)$$

with (dimensionless) parameters $m_\infty = 3.307$, $c = 2.187$, based on the LQCD calculation in Ref. [62] and fixing c to the $N_c = 3$ result. We also take $\sigma = 0.18$ GeV².

The general trend can easily be understood by studying the second Landau parameter (40). For model B, it reads

$$\bar{u}_2 \approx \frac{N_c^2}{\pi^2} \left(1 - 3 \frac{1}{2} \left(\frac{m_A}{T} \right)^2 K_2(m_A/T) \right). \quad (88)$$

Solving for $m_A(N_c)$ from

$$\bar{u}_2(m_A(N_c), T = T_d(N_c)) = 0, \quad (89)$$

we obtain the gray dashed line in Fig. 6 (right). Equation (88) suggests that the leading N_c dependence comes not from the prefactor but from the N_c dependence of T_d .⁷ While it is not surprising that the observables are related, the effective model offers a simple approximate connection such as (88).

⁷Relation (88) assumes the Boltzmann approximation. This may be justified for the massive gluons, but may not be the case for the ghost. The corrections, however, are N_c dependent. For $N_c = 3$, this amounts to replacing $1 \rightarrow \frac{\pi^2}{9} \approx 1.097$ in the right bracket. The corresponding result for $N_c = 2$ is $1 \rightarrow \frac{\pi^2}{12} \approx 0.822$.

V. CONCLUSION

We have examined the fluctuations of the order parameter, measured by the Polyakov loop susceptibilities in the $SU(N_c)$ pure gauge theory, using an effective potential built from one-loop expressions of the field determinants of gluon and ghost. The connection between these observables with the Cartan angles and their curvature masses are derived. The latter can serve as a proxy for the A_0 -gluon screening mass and are strongly influenced by the $Z(N_c)$ structure of the vacuum.

The Cartan curvature masses thus provide useful diagnostic information concerning the competition of gluons and ghosts in the QCD medium. While we expect gauge invariance for all observables based on the Polyakov loops, it is unlikely for the model potential in the current state to achieve this goal. For example, we see that the predictions of these curvature masses depend strongly on the assumptions of the gluon and ghost propagators, and the choice of gauge. Another essential limitation of the present model is that the propagators and wave function renormalizations we fitted are not LQCD computation in the background-field gauge. A more constructive way to proceed is to explore the potential, and more generally the problem of how confinement manifests, in various gauges, and check whether there could be nontrivial relations among the model parameters such that the gauge dependence would be removed or reduced when computing physical observables.

A natural progression of this work is a consistent treatment of the finite temperature behaviors of m_A and the wave function renormalizations within the model. A crude assessment gives the following competing effects: (1) slightly (Boltzmann-)suppressed deconfining force from transverse

gluons due to an increased m_A at finite temperatures, (2) an increase in confining force by the ghost due to the enhanced ghost form factor, (3) an increase in deconfining force from the longitudinal gluons due to the characteristic dip in m_{A_0} . It is possible that while T_d would not be strongly affected, the curvature masses will be substantially modified.

What is clear from the model study is that the longitudinal gluon propagator and the Cartan curvature masses are connected [via Eqs. (71) and (78)], and should be determined self-consistently in model calculations. This makes for a more meaningful comparison with the finite temperature LQCD data [54,63–65]. For the transverse gluons, we find no evidence for a substantial change in their masses across the phase transition, nor the need for the value to approach infinity in the confined phase. In fact, they serve as constituents of the glueballs.

A possible future application of the relations between the Polyakov loop observables with those from the gluon propagators could be in formulating a nonperturbative renormalization scheme for the former as composite operators. This is a necessary first step to properly compare effective model results with LQCD data of the Polyakov loops and the susceptibilities. This will be explored in a future work.

ACKNOWLEDGMENTS

P. M. L. thanks O. Oliveira for stimulating discussions. We acknowledge the support by the Polish National Science Center (NCN) under Opus Grant No. 2018/31/B/ST2/01663. K. R. also acknowledges partial support of the Polish Ministry of Science and Higher Education.

-
- [1] G. Boyd, J. Engels, F. Karsch, E. Laermann, C. Legeland, M. Lutgemeier, and B. Petersson, Thermodynamics of $SU(3)$ lattice gauge theory, *Nucl. Phys.* **B469**, 419 (1996).
 - [2] S. Borsanyi, G. Endrodi, Z. Fodor, S. D. Katz, and K. K. Szabo, Precision $SU(3)$ lattice thermodynamics for a large temperature range, *J. High Energy Phys.* **07** (2012) 056.
 - [3] O. Kaczmarek, F. Karsch, P. Petreczky, and F. Zantow, Heavy quark anti-quark free energy and the renormalized Polyakov loop, *Phys. Lett. B* **543**, 41 (2002).
 - [4] K. Fukushima and C. Sasaki, The phase diagram of nuclear and quark matter at high baryon density, *Prog. Part. Nucl. Phys.* **72**, 99 (2013).
 - [5] K. Fukushima and V. Skokov, Polyakov loop modeling for hot QCD, *Prog. Part. Nucl. Phys.* **96**, 154 (2017).
 - [6] J. O. Andersen, W. R. Naylor, and A. Tranberg, Phase diagram of QCD in a magnetic field: A review, *Rev. Mod. Phys.* **88**, 025001 (2016).
 - [7] F. Bruckmann, G. Endrodi, and T. G. Kovacs, Inverse magnetic catalysis and the Polyakov loop, *J. High Energy Phys.* **04** (2013) 112.
 - [8] E. S. Fraga, B. W. Mintz, and J. Schaffner-Bielich, A search for inverse magnetic catalysis in thermal quark-meson models, *Phys. Lett. B* **731**, 154 (2014).
 - [9] V. P. Pagura, D. Gomez Dumm, S. Noguera, and N. N. Scoccola, Magnetic catalysis and inverse magnetic catalysis in nonlocal chiral quark models, *Phys. Rev. D* **95**, 034013 (2017).
 - [10] P. M. Lo, M. Szymański, K. Redlich, and C. Sasaki, Polyakov loop fluctuations in the presence of external fields, *Phys. Rev. D* **97**, 114006 (2018).

- [11] P.M. Lo, M. Szymański, C. Sasaki, and K. Redlich, Deconfinement in the presence of a strong magnetic field, *Phys. Rev. D* **102**, 034024 (2020).
- [12] C. Ratti, M. A. Thaler, and W. Weise, Phases of QCD: Lattice thermodynamics and a field theoretical model, *Phys. Rev. D* **73**, 014019 (2006).
- [13] A. Dumitru, Y. Guo, Y. Hidaka, C.P. Altes, and R.D. Pisarski, Effective matrix model for deconfinement in pure gauge theories, *Phys. Rev. D* **86**, 105017 (2012).
- [14] P.M. Lo, B. Friman, O. Kaczmarek, K. Redlich, and C. Sasaki, Polyakov loop fluctuations in SU(3) lattice gauge theory and an effective gluon potential, *Phys. Rev. D* **88**, 074502 (2013).
- [15] U. Reinosa, J. Serreau, M. Tissier, and N. Wschebor, Deconfinement transition in SU(N) theories from perturbation theory, *Phys. Lett. B* **742**, 61 (2015).
- [16] J. Braun, H. Gies, and J. M. Pawłowski, Quark confinement from color confinement, *Phys. Lett. B* **684**, 262 (2010).
- [17] P.N. Meisinger, T.R. Miller, and M. C. Ogilvie, Phenomenological equations of state for the quark gluon plasma, *Phys. Rev. D* **65**, 034009 (2002).
- [18] P.N. Meisinger, M. C. Ogilvie, and T.R. Miller, Gluon quasiparticles and the polyakov loop, *Phys. Lett. B* **585**, 149 (2004).
- [19] P. Alba, W. Alberico, M. Bluhm, V. Greco, C. Ratti, and M. Ruggieri, Polyakov loop and gluon quasiparticles: A self-consistent approach to Yang–Mills thermodynamics, *Nucl. Phys. A* **934**, 41 (2014).
- [20] V. M. Bannur, Self-consistent quasiparticle model for quark-gluon plasma, *Phys. Rev. C* **75**, 044905 (2007).
- [21] J. Braun, A. Eichhorn, H. Gies, and J. M. Pawłowski, On the nature of the phase transition in SU(N), Sp(2) and E(7) Yang-Mills theory, *Eur. Phys. J. C* **70**, 689 (2010).
- [22] C. Sasaki and K. Redlich, An effective gluon potential and hybrid approach to Yang-Mills thermodynamics, *Phys. Rev. D* **86**, 014007 (2012).
- [23] K. Fukushima and K. Kashiwa, Polyakov loop and QCD thermodynamics from the gluon and ghost propagators, *Phys. Lett. B* **723**, 360 (2013).
- [24] P.M. Lo, B. Friman, O. Kaczmarek, K. Redlich, and C. Sasaki, Probing deconfinement with Polyakov loop susceptibilities, *Phys. Rev. D* **88**, 014506 (2013).
- [25] C. Sasaki, B. Friman, and K. Redlich, Susceptibilities and the phase structure of a chiral model with Polyakov loops, *Phys. Rev. D* **75**, 074013 (2007).
- [26] P.M. Lo, B. Friman, and K. Redlich, Polyakov loop fluctuations and deconfinement in the limit of heavy quarks, *Phys. Rev. D* **90**, 074035 (2014).
- [27] K. Fukushima, Chiral effective model with the Polyakov loop, *Phys. Lett. B* **591**, 277 (2004).
- [28] D. Zwanziger, Equation of State of Gluon Plasma from Fundamental Modular Region, *Phys. Rev. Lett.* **94**, 182301 (2005).
- [29] A. Szczepaniak, E. S. Swanson, C.-R. Ji, and S. R. Cotanch, Glueball Spectroscopy in a Relativistic Many Body Approach to Hadron Structure, *Phys. Rev. Lett.* **76**, 2011 (1996).
- [30] H. Georgi, *Lie Algebras in Particle Physics. From Isospin to Unified Theories*, Vol. 54 (CRC Press, UK, 1982), <https://doi.org/10.1201/9780429499210>.
- [31] D. J. Gross, R. D. Pisarski, and L. G. Yaffe, QCD and instantons at finite temperature, *Rev. Mod. Phys.* **53**, 43 (1981).
- [32] A. Dumitru, Y. Guo, and C. P. K. Altes, Two-loop perturbative corrections to the thermal effective potential in gluodynamics, *Phys. Rev. D* **89**, 016009 (2014).
- [33] N. Weiss, The effective potential for the order parameter of gauge theories at finite temperature, *Phys. Rev. D* **24**, 475 (1981).
- [34] A. Gocksch and R. D. Pisarski, Partition function for the eigenvalues of the Wilson line, *Nucl. Phys. B* **402**, 657 (1993).
- [35] L. von Smekal, A. Hauck, and R. Alkofer, A solution to coupled Dyson–Schwinger equations for gluons and ghosts in Landau gauge, *Ann. Phys. (N.Y.)* **267**, 1 (1998); Erratum: *Ann. Phys. (N.Y.)* **269**, 182 (1998).
- [36] L. von Smekal, R. Alkofer, and A. Hauck, The Infrared Behavior of Gluon and Ghost Propagators in Landau Gauge QCD, *Phys. Rev. Lett.* **79**, 3591 (1997).
- [37] C. S. Fischer, A. Maas, and J. M. Pawłowski, On the infrared behavior of Landau gauge Yang-Mills theory, *Ann. Phys. (Amsterdam)* **324**, 2408 (2009).
- [38] A. C. Aguilar, D. Binosi, and J. Papavassiliou, Gluon and ghost propagators in the Landau gauge: Deriving lattice results from Schwinger-Dyson equations, *Phys. Rev. D* **78**, 025010 (2008).
- [39] L. Fister and J. M. Pawłowski, Confinement from correlation functions, *Phys. Rev. D* **88**, 045010 (2013).
- [40] C. S. Fischer, J. Luecker, and C. A. Welzbacher, Phase structure of three and four flavor QCD, *Phys. Rev. D* **90**, 034022 (2014).
- [41] A. K. Cyrol, M. Mitter, J. M. Pawłowski, and N. Strodthoff, Nonperturbative finite-temperature Yang-Mills theory, *Phys. Rev. D* **97**, 054015 (2018).
- [42] A. Maas, Describing gauge bosons at zero and finite temperature, *Phys. Rep.* **524**, 203 (2013).
- [43] P.M. Lo and E. S. Swanson, Confinement models at finite temperature and density, *Phys. Rev. D* **81**, 034030 (2010).
- [44] C. W. Bernard, Feynman rules for gauge theories at finite temperature, *Phys. Rev. D* **9**, 3312 (1974).
- [45] I. Bogolubsky, E. Ilgenfritz, M. Müller-Preussker, and A. Sternbeck, Lattice gluodynamics computation of Landau gauge Green’s functions in the deep infrared, *Phys. Lett. B* **676**, 69 (2009).
- [46] R. Alkofer and L. von Smekal, The infrared behavior of QCD Green’s functions: Confinement dynamical symmetry breaking, and hadrons as relativistic bound states, *Phys. Rep.* **353**, 281 (2001).
- [47] T. Iritani, H. Suganuma, and H. Iida, Gluon-propagator functional form in the Landau gauge in SU(3) lattice QCD: Yukawa-type gluon propagator and anomalous gluon spectral function, *Phys. Rev. D* **80**, 114505 (2009).
- [48] A. Maas, Dependence of the propagators on the sampling of Gribov copies inside the first Gribov region of Landau gauge, *Ann. Phys. (Amsterdam)* **387**, 29 (2017).
- [49] A. Maas, Constraining the gauge-fixed Lagrangian in minimal Landau gauge, *SciPost Phys.* **8**, 071 (2020).
- [50] D. Dudal, O. Oliveira, and P. J. Silva, High precision statistical Landau gauge lattice gluon propagator computa-

- tion vs. the Gribov–Zwanziger approach, *Ann. Phys. (Amsterdam)* **397**, 351 (2018).
- [51] A. F. Falcão, O. Oliveira, and P. J. Silva, Analytic structure of the lattice Landau gauge gluon and ghost propagators, *Phys. Rev. D* **102**, 114518 (2020).
- [52] N. Weiss, The Wilson line in finite temperature gauge theories, *Phys. Rev. D* **25**, 2667 (1982).
- [53] A. Dumitru and R. D. Pisarski, Degrees of freedom and the deconfining phase transition, *Phys. Lett. B* **525**, 95 (2002).
- [54] P. J. Silva, O. Oliveira, P. Bicudo, and N. Cardoso, Gluon screening mass at finite temperature from the Landau gauge gluon propagator in lattice QCD, *Phys. Rev. D* **89**, 074503 (2014).
- [55] A. Maas, J. M. Pawłowski, L. von Smekal, and D. Spielmann, The Gluon propagator close to criticality, *Phys. Rev. D* **85**, 034037 (2012).
- [56] U. Reinosa, J. Serreau, M. Tissier, and N. Wschebor, Two-loop study of the deconfinement transition in Yang-Mills theories: SU(3) and beyond, *Phys. Rev. D* **93**, 105002 (2016).
- [57] K. Langfeld and L. Moyaerts, Propagators in Coulomb gauge from SU(2) lattice gauge theory, *Phys. Rev. D* **70**, 074507 (2004).
- [58] D. Dudal, S. P. Sorella, N. Vandersickel, and H. Verschelde, New features of the gluon and ghost propagator in the infrared region from the Gribov-Zwanziger approach, *Phys. Rev. D* **77**, 071501 (2008).
- [59] A. P. Szczepaniak and E. S. Swanson, Coulomb gauge QCD, confinement, and the constituent representation, *Phys. Rev. D* **65**, 025012 (2001).
- [60] G. Lacroix, C. Semay, D. Cabrera, and F. Buisseret, Glueballs and the Yang-Mills plasma in a T-matrix approach, *Phys. Rev. D* **87**, 054025 (2013).
- [61] B. Lucini, A. Rago, and E. Rinaldi, SU(N_c) gauge theories at deconfinement, *Phys. Lett. B* **712**, 279 (2012).
- [62] B. Lucini, M. Teper, and U. Wenger, Glueballs and k-strings in SU(N) gauge theories: Calculations with improved operators, *J. High Energy Phys.* **06** (2004) 012.
- [63] R. Aouane, V. Bornyakov, E. Ilgenfritz, V. Mitrjushkin, M. Müller-Preussker, and A. Sternbeck, Landau gauge gluon and ghost propagators at finite temperature from quenched lattice QCD, *Phys. Rev. D* **85**, 034501 (2012).
- [64] V. G. Bornyakov and V. K. Mitrjushkin, SU(2) lattice gluon propagators at finite temperatures in the deep infrared region and Gribov copy effects, *Phys. Rev. D* **84**, 094503 (2011).
- [65] P. Bicudo, N. Cardoso, and M. Cardoso, Pure gauge QCD flux tubes and their widths at finite temperature, *Nucl. Phys.* **B940**, 88 (2019).